Neuron, Vol. 49, 671–682, March 2, 2006 ©2006 Elsevier Inc. DOI 10.1016/j.neuron.2006.01.020

M1 Receptors Play a Central Role in Modulating AD-like Pathology in Transgenic Mice

Antonella Caccamo,[1] Salvatore Oddo,[1] Lauren M. Billings,[1] Kim N. Green,[1] Hilda Martinez-Coria,[1] Abraham Fisher,[2] and Frank M. LaFerla[1,*]

[1] Department of Neurobiology and Behavior
University of California, Irvine
Irvine, California 92697

[2] Israel Institute for Biological Research
Ness-Ziona, 74100
Israel

Summary

We investigated the therapeutic efficacy of the selective M1 muscarinic agonist AF267B in the 3xTg-AD model of Alzheimer disease. AF267B administration rescued the cognitive deficits in a spatial task but not contextual fear conditioning. The effect of AF267B on cognition predicted the neuropathological outcome, as both the Aβ and tau pathologies were reduced in the hippocampus and cortex, but not in the amygdala. The mechanism underlying the effect on the Aβ pathology was caused by the selective activation of ADAM17, thereby shifting APP processing toward the nonamyloidogenic pathway, whereas the reduction in tau pathology is mediated by decreased GSK3β activity. We further demonstrate that administration of dicyclomine, an M1 antagonist, exacerbates the Aβ and tau pathologies. In conclusion, AF267B represents a peripherally administered low molecular weight compound to attenuate the major hallmarks of AD and to reverse deficits in cognition. Therefore, selective M1 agonists may be efficacious for the treatment of AD.

Introduction

Alzheimer's disease (AD) is the most common neurodegenerative disorder afflicting the elderly, causing progressive memory loss and cognitive dysfunction. Neuropathologically, the AD brain is characterized by two hallmark proteinaceous aggregates, amyloid plaques, mainly composed of the amyloid-β peptide (Aβ); and neurofibrillary tangles, comprised of hyperphosphorylated aggregates of the tau protein (Selkoe, 2001). Aβ is derived via proteolysis from the amyloid precursor protein (APP). APP is processed in two different ways: a nonamyloidogenic pathway, where an α-secretase enzyme cleaves APP in the middle of the Aβ sequence, thereby precluding Aβ formation; and an amyloidogenic pathway, in which APP is sequentially cut by β- and γ-secretase, leading to Aβ formation. The buildup of Aβ is considered to be a central feature in the pathogenesis of AD (Hardy and Selkoe, 2002). However, other critical molecular and neurochemical alterations occur as well. Of these, cholinergic dysfunction is particularly relevant, as it occurs early in the disease process (Davies and Maloney, 1976; Muir, 1997) and the majority of the FDA-approved therapies for AD are aimed at improving cholinergic function (Ibach and Haen, 2004).

Acetylcholine (ACh), a key neurotransmitter involved with learning and memory (Woolf, 1996), binds to two distinct receptor subtypes in the brain: nicotinic (nAChR) and muscarinic (mAChR). Whereas nAChRs are ligand-gated ion channels, mAChRs are metabotropic receptors. Five distinct mAChR subtypes (M1–M5), each encoded by a different gene, have been identified in the CNS (Levey et al., 1991; Wei et al., 1994). The M1 mAChR is the most abundant subtype in the cortex and hippocampus, two main brain regions that develop plaques and tangles, rendering it an attractive therapeutic target for restoring cholinergic function (Levey et al., 1991; Wei et al., 1994). The first generation of muscarinic agonists, however, failed during clinical trials, mostly due to narrow safety margins, low bioavailability, low intrinsic activity, and lack of selectivity for the M1 mAChR (Eglen et al., 2001). A second generation of selective M1 agonists has recently been developed that overcomes these limitations. Among these, AF267B is a selective M1 muscarinic agonist capable of crossing the blood-brain barrier, although the therapeutic efficacy of these new M1 agonists on Aβ and tau pathologies and the associated cognitive impairments has yet not been addressed in vivo.

Transgenic mice have proven highly valuable for evaluating putative AD therapies (Cuajungco et al., 2000; DeMattos et al., 2001; Jankowsky et al., 2002; Janus et al., 2001; Riekkinen et al., 1998; Schenk et al., 1999). We previously reported the generation of a transgenic model of AD (3xTg-AD) that progressively manifests several disease-relevant features, including plaques, tangles, cholinergic dysfunction, and cognitive impairments (Billings et al., 2005; Oddo et al., 2003, 2005). Evaluation of potential therapeutic compounds in a model with both plaques and tangles is highly desirable, as a compound may have opposite effects on the Aβ and tau pathology (Oddo et al., 2004, 2005). Notably, some transgenic studies have shown that the cholinergic nicotinic agonist nicotine can ameliorate the Aβ pathology in APP transgenic mice with well established plaques (Nordberg et al., 2002), whereas our own recent study in the 3xTg-AD mice shows that it also exacerbates the tau pathology (Oddo et al., 2005), thereby raising doubts about the utility of nonselective nicotinic agonists as a viable treatment for AD. In the present study, we explored the efficacy of a selective M1 agonist on the Aβ and tau neuropathology and cognitive decline. We also investigated the effect of the M1 antagonist dicyclomine on these parameters as well.

Results

To evaluate the therapeutic efficacy of a selective M1 agonist on the neuropathological and cognitive phenotype, we chronically administered AF267B to 6-month-old NonTg and 3xTg-AD homozygous mice (n = 8/group).

*Correspondence: laferla@uci.edu

As a proof of principle, we evaluated the consequences that exposure to the M1 mAChRs antagonist dicyclomine (Giachetti et al., 1986) had on the AD pathology and cognitive phenotype of these mice. Accordingly, we treated 6-month-old 3xTg-AD homozygous mice (n = 10) for 4 weeks with the selective M1 antagonist dicyclomine (8 mg/kg). At this age, the 3xTg-AD mice show impaired spatial and contextual memory (Billings et al., 2005) and neuropathologically harbor diffuse plaques, accumulation of intraneuronal Aβ, and somatodendritic compartmentalization of tau (Oddo et al., 2003). The mice were given daily intraperitoneal (i.p.) injections of AF267B for 10 weeks at a low or high dose (1 mg/kg/day or 3 mg/kg/day, respectively), or they received the muscarinic antagonist dicyclomine (8 mg/kg) for 4 weeks, whereas the control group was provided with vehicle only (PBS) (see Table S1 in the Supplemental Data available online). As we did not find any statistically significant differences between the mice treated with 1 or 3 mg/kg of AF267B, we pooled all the data from the AF267B-treated mice. We carefully monitored the general health of the mice throughout the course of the treatment and did not observe any adverse changes nor did we observe significant weight changes (Table S1).

AF267B Ameliorates Spatial Learning and Memory Impairments, and Exacerbation by Dicyclomine

After 8 weeks of daily AF267B administration and 4 weeks of daily injection of dicyclomine, we evaluated the effects of modulating the cholinergic system on learning and memory using two different behavioral paradigms: Morris water maze and passive inhibitory avoidance. These tasks are mainly dependent on the hippocampus and amygdala, respectively, and were selected because the amyloid and tangle pathology initially manifests, and is most severe, in the hippocampus, cortex, and amygdala in the 3xTg-AD mice (Oddo et al., 2003). Both compounds were also administered during the 2 weeks of behavioral testing.

Mice were trained to criterion (escape latency <20 s) in the spatial reference version of the Morris water maze to find the location of a hidden platform. Whereas PBS- and AF267B-treated NonTg mice reached criterion in 4 days, PBS-treated 3xTg-AD mice required 6 days, but notably they were still able to learn the task (Figure 1A). AF267B-treated 3xTg-AD mice reached criterion after 4 days, thereby paralleling the performance of NonTg mice, which was unaffected by this treatment (Figure 1A). In contrast, both 3xTg-AD and NonTg mice treated with dicyclomine showed a slower learning curve and reached criterion after 6 days (Figure 1A). As we have previously shown, the 3xTg-AD mice require extra training to reach criterion due to the inability to remember the acquired information between days of training (Billings et al., 2005). We therefore evaluated the performance of each group on a trial-by-trial basis. In contrast to the NonTg mice treated with AF267B or PBS, PBS-treated 3xTg-AD mice and dicyclomine-treated 3xTg-AD and NonTg mice showed significantly longer escape latencies at the first trial of each day compared to the last trial the previous day (Figure 1B). Thus, the poorer performance was due to a day-to-day impairment in retention or retrieval. Most notably, AF267B treatment rescued the day-to-day retention deficit in the 3xTg-AD mice (Figure 1B).

To determine the effects of modulating the cholinergic system on short- and long-term memory, probe trials were conducted 1.5 and 24 hr after the last training trail, respectively. Once again, AF267B did not influence memory in the NonTg mice but significantly rescued the memory impairments in the 3xTg-AD mice, as determined by the marked reduction in the latency to cross the platform, number of platform location crosses, and the time spent in the opposite quadrant (Figures 1C–1E). In contrast, dicyclomine exacerbated the cognitive impairments in all the measurements (Figures 1C–1E). Notably, the memory impairments were worse in dicyclomine-treated 3xTg-AD mice compared to dicyclomine-treated NonTg mice (Figures 1C–1E).

We next evaluated the effect of modulating the cholinergic system on a contextual learning and memory task using passive inhibitory avoidance, a task primarily dependent on the amygdala (McGaugh et al., 2002). Whereas NonTg mice effectively avoided the dark, shock-associated compartment, all the 3xTg-AD mice (including the AF267B-treated mice) showed impaired short- and long-term memory (Figure 1F). Therefore, AF267B treatment rescued the cognitive deficits in spatial learning but did not effectively rescue impairments on a contextual, amygdala-dependent task in the 3xTg-AD mice (see below for explanation). In contrast, both 3xTg-AD and NonTg mice treated with dicyclomine showed a statistically significant reduction in the latency to enter the dark compartment during both probe trials (Figure 1F).

Aβ Levels Are Reduced by AF267B but Increased by Dicyclomine

All mice were sacrificed 24 hr after the last trial on the passive inhibitory avoidance, and their brains were isolated and processed for neuropathological or biochemical evaluation. We first analyzed the steady-state levels of the M1 mAChRs in all the groups of mice by quantitative Western blot. Chronic AF267B or dicyclomine exposure did not cause any discernible alteration in the steady-state levels of M1 mAChRs in either NonTg or 3xTg-AD mice (Figure 2). It is also important to note that the constitutive levels of the M1 receptor were comparable between PBS-treated 3xTg-AD and NonTg mice. This finding is consistent with previous reports showing that there is a selective loss of nicotinic receptors but not muscarinic receptors in the AD brain (Nordberg et al., 1992; Nordberg and Winblad, 1986; Sugaya et al., 1990; Whitehouse et al., 1986). The data presented here, together with our previous finding showing that the 3xTg-AD mice have an age-dependent loss of α7nAChRs (Oddo et al., 2005), indicate that the 3xTg-AD mice also mimic this feature of AD neuropathology.

To determine the consequences of AF267B treatment on Aβ deposition, we immunostained sections from treated and untreated 3xTg-AD mice with different anti-Aβ antibodies. At 8 months of age, the homozygous 3xTg-AD mice typically show widespread intraneuronal Aβ accumulation throughout the cortex, hippocampus, and the amygdala and diffuse plaques in specific cortical regions and in the CA1/subiculum region. Following AF267B administration, we observed a marked

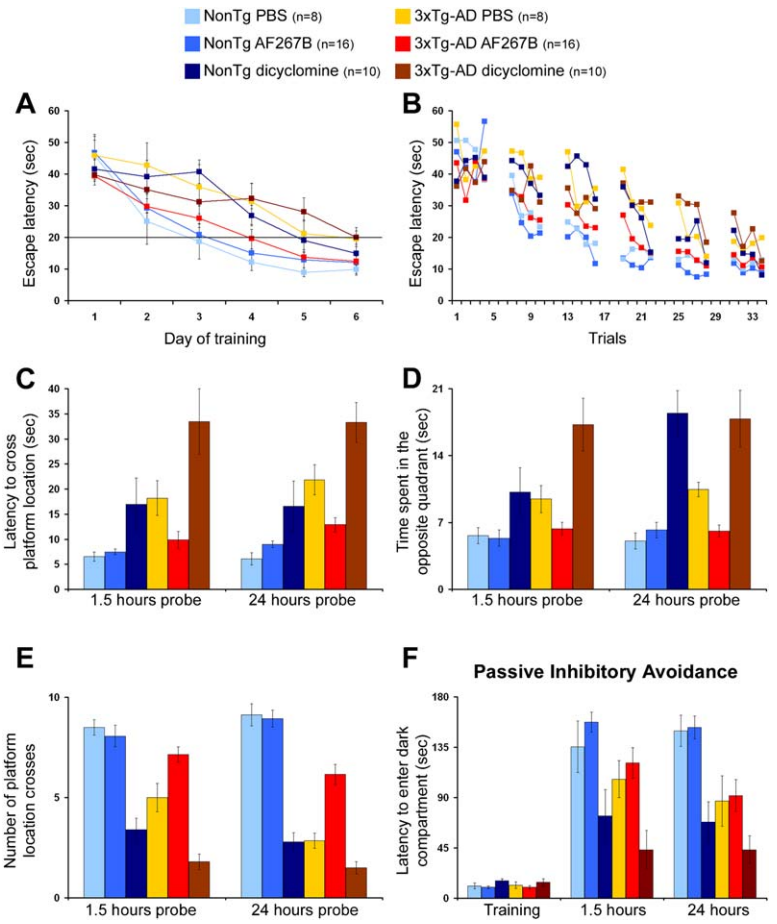

Figure 1. AF267B Rescues Memory Impairments in a Hippocampal- but not Amygdala-Dependent Task in the 3xTg-AD Mice

3xTg-AD and NonTg mice given vehicle (PBS), dicyclomine, or AF267B were trained and tested on the spatial memory version of the Morris water maze (MWM) as well as inhibitory avoidance (IA).

(A and B) AF267B rescues spatial memory retention deficits during training. All mice were trained to criterion in the MWM task (indicated by solid lines at 20 s escape latency). Whereas PBS-treated 3xTg-AD mice require more training to reach criterion in the MWM compared to NonTg mice ($p < 0.05$ at days 2, 3, and 4 of training), mice given AF267B showed no significant differences during training compared to NonTg mice (A). Indeed, AF267B treatment ameliorated the day-to-day retention deficits exhibited by PBS-treated 3xTg-AD homozygous mice (B). In contrast, dicyclomine-treated mice required more time to learn the task compared to genotype-matched PBS-treated mice.

(C–E) AF267B rescues short- and long-term spatial memory deficits in probe trials. Mice were given a memory probe with the platform removed 1.5 or 24 hr following the last training trial. Compared to PBS-treated 3xTg-AD mice, 3xTg-AD mice given AF267B exhibited significantly decreased latencies to cross the platform location ($p < 0.05$; $t = 3.871$ and $P < 0.05$; $t = 3.014$, for the 1.5 and 24 hr probe, respectively) (C), time in the opposite quadrant ($p < 0.05$; $t = 3.371$ and $P < 0.05$; $t = 3.380$, for the 1.5 and 24 hr probe, respectively) (D), as well as significantly higher numbers of platform location crosses ($p < 0.05$; $t = 3.251$ and $p < 0.001$; $t = 4.804$, for the 1.5 and 24 hr probe, respectively) (E). In contrast, dicyclomine-treated 3xTg-AD mice performed worse relative to PBS-treated 3xTg-AD mice in latencies to cross the platform location ($p < 0.05$; $t = 3.683$ and $P < 0.05$; $t = 3.571$, for the 1.5 and 24 hr probe, respectively) (C), time in the opposite quadrant ($p < 0.05$; $t = 3.154$ and $P < 0.05$; $t = 3.892$, for the 1.5 and 24 hr probe, respectively) (D), and had significantly higher numbers of platform location crosses ($p < 0.05$; $t = 3.742$ and $P < 0.01$; $t = 4.001$, for the 1.5 and 24 hr probe, respectively).

(F) Differential effect of dicyclomine and AF267B on contextual fear memory. Mice were placed in a light compartment and received a mild foot shock upon crossing over to the dark compartment. Mice were tested for retention of memory for fear-associated environments 1.5 and 24 hr after training. Notably, AF267B had no effect on contextual fear memory, as no statistical significance was observed in the latency to enter the dark compartment between PBS- and AF267B-treated mice. The latency to enter the dark compartment during the 1.5 and 24 hr probe trial was significantly lower for the dicyclomine-treated mice compared to PBS- and AF267B-treated mice, indicating that dicyclomine administration further impaired conditional fear memory in both the 3xTg-AD and NonTg mice ($p < 0.05$; $t = 2.951$ and $P < 0.05$; $t = 3.024$, for the 1.5 and 24 hr probe, respectively).

reduction in both intracellular and extracellular Aβ immunoreactivity in the cortex and hippocampus (Figures 3A and 3B and 3D and 3E, respectively, and Figure 3J). Notably, we did not observe any significant changes in the level of Aβ immunoreactivity in the amygdala of PBS-treated versus AF267B-treated 3xTg-AD mice (Figures 3G and 3H). In contrast, dicyclomine administration exacerbated the Aβ pathology in all three brain regions (Figures 3C, 3F, 3I, and 3J). It is important to note that the AF267B-mediated reduction in Aβ pathology in the hippocampus, but not in the amygdala, is predicted by the behavioral data, as AF267B treatment rescued the cognitive deficit in a hippocampal-dependent task but not in an amygdala-dependent task.

To quantitatively assess the effect on Aβ levels, we next assayed the brains by sandwich ELISA and found no effect on SDS-soluble Aβ1-40 levels between AF267B-treated and PBS-treated 3xTg-AD mice (Figure 3K). In contrast, we observed a significant decrease in Aβ1-42 levels in both the SDS- and formic acid (FA)-soluble fractions (Figure 3K). As expected, based on the immunohistochemical data, we found a general increase in the Aβ levels in the dicyclomine-treated 3xTg-AD mice (Figure 3K). Note, we cannot detect FA-soluble Aβ1-40 at this age in the 3xTg-AD mice. Consequently, the amelioration of the Aβ pathology in the cortex and hippocampus of the AF267B-treated 3xTg-AD mice is probably due to a selective reduction in Aβ1-42. The reason for such a selective reduction of Aβ1-42 without an effect on Aβ1-40 may be due to an indirect inhibitory effect on γ-secretase following activation of M1 mAChRs (Nitsch et al., 1992).

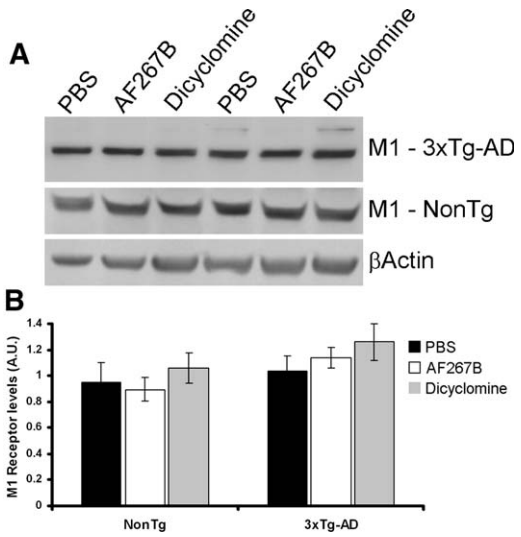

Figure 2. Steady-State Levels of the M1 mAChRs Are Unaltered following AF267B or Dicyclomine Treatment

We measured the M1 mAChR levels in NonTg and 3xTg-AD mice treated either with PBS, dicyclomine, or AF267B using quantitative Western blot. (A) Representative Western blot probed with a specific antibody against M1 mAChRs. β-actin levels were used to control for the protein loading. Panel (B) shows quantitative analysis of the M1 mAChR levels in NonTg and 3xTg-AD mice treated with PBS, dicyclomine, or AF267B. Neither dicyclomine nor AF267B had any effect of the M1 receptor levels. Moreover, we did not find any difference when compared the M1 levels between PBS-treated NonTg and 3xTg-AD mice ($p > 0.05$). The graph represents the mean of the M1 receptor levels measured in eight mice per group. The error bar indicates the standard error.

AF267B and Dicyclomine Inversely Modulate APP Processing

To elucidate the mechanism responsible for the reduction in Aβ following AF267B administration, we analyzed APP processing by Western blot analysis. We first analyzed the levels of full-length APP from PBS-, AF267B-, and dicyclomine-treated 3xTg-AD mice using 22C11 (an N-terminal-specific APP antibody) and found that APP steady-state levels were not significantly altered by either of these treatments (Figures 4A and 4B). To investigate the steady-state levels of the major C-terminal derivatives, protein extracts were probed with CT20, a C-terminal-specific APP antibody (Pinnix et al., 2001). We found a significant reduction in the steady-state levels of C99 that coincides with a concomitant and significant increase in C83 levels in the brains of AF267B-treated 3xTg-AD mice (Figures 4A and 4B). In contrast, the levels of C99 were higher, but did not reach statistical significance between PBS- and dicyclomine-treated mice (Figures 4A and 4B). The dicyclomine-mediated increase in C99 levels was followed by a statistically significant decrease in C83 levels (Figures 4A and 4B). Therefore, these data indicate that this selective M1 agonist increases formation of the α-secretase-generated C83 fragment in the brains of the 3xTg-AD mice, whereas its levels are lower following treatment with the M1 antagonist.

To elucidate the mechanism underlying the changes in APP processing, we compared the levels of ADAM10 and ADAM17/TACE, two putative α-secretase enzymes (Allinson et al., 2003; Lammich et al., 1999; Postina et al., 2004); and the β-APP cleaving enzyme BACE1 (Vassar et al., 1999) between PBS-, AF267B-, and dicyclomine-treated 3xTg-AD mice. We found no changes in ADAM10 steady-state levels following AF267B or dicyclomine treatments; however, we found a selective increase in the steady-state levels of ADAM17/TACE in the brains of AF267B-treated mice (Figures 4C and 4D). Conversely, we found a significant decrease in BACE1 levels in the brains of AF267B-treated versus untreated 3xTg-AD mice (Figures 4E and 4F). Notably, BACE1 levels were significantly higher in the dicyclomine-treated mice compared with PBS-injected mice (Figures 4E and 4F). The selective increase in ADAM17 following AF267B administration is consistent with previous reports indicating that this α-secretase enzyme is inducible by muscarine, whereas ADAM10 is the major constitutive enzyme (Allinson et al., 2003). Furthermore, previous in vitro studies have shown that activation of M1 mAChRs activates α-secretase (Allinson et al., 2003; Buxbaum et al., 1992; Haring et al., 1998; Nitsch et al., 1992). Although a change in the steady-state levels does not always reflect changes in activity, these data, together with the changes in the levels of C99, C83, and Aβ, strongly suggest that the effects on Aβ pathology following AF267B treatment are due to a shift in the APP processing toward the nonamyloidogenic pathway.

Increase in ERK1/2 and PKC Activities following AF267B Treatment

In vitro evidence suggests that PKC and ERK1/2 may mediate the M1-modulation of APP processing (Bigl and Rossner, 2003). To determine if PKC and ERK1/2 underlie the AF267B-induced increase in α-secretase activity in vivo, we compared the activity of PKC and ERK1/2 in the brains of AF267B- and dicyclomine-treated versus PBS-treated 3xTg-AD mice. Using quantitative Western blot analysis, we found that the levels of ERK1/2 were not changed following AF267B or dicyclomine treatment (Figures 5A and 5B). Notably, using an anti-ERK1/2 antibody raised against phosphorylated ERK1/2 at residues T185/Y187, we found a marked and significant increase in the levels of phosphorylated ERK1/2 in the brains of AF267B-treated compared to PBS-treated mice (Figures 5A and 5B). In contrast, the levels of phosphorylated ERK1/2 were significantly reduced in the brains of dicyclomine-treated 3xTg-AD mice (Figures 5A and 5B). Considering that an increase in ERK1/2 phosphorylation is thought to reflect of an increase in its activity (Sugden and Clerk, 1997), the data presented here clearly show that the cholinergic system can effectively modulate the activity of these enzymes in vivo and suggest that the AF267B-mediated modulation of APP processing is, at least in part, mediated by changes in the activity of ERK1/2. Our results are consistent with in vitro studies showing that the stimulation of M1 receptors by carbacol (a cholinergic agonist) leads to an increase in the activity of ERK1/2 in a dose-dependent fashion (Rosenblum et al., 2000).

To determine if the activity of PKC changes following cholinergic modulation, we also measured its enzymatic activity in the brains of PBS-, AF267B-, and dicyclomine-treated 3xTg-AD mice. We found a significant increase in the activity of PKC following AF267B administration

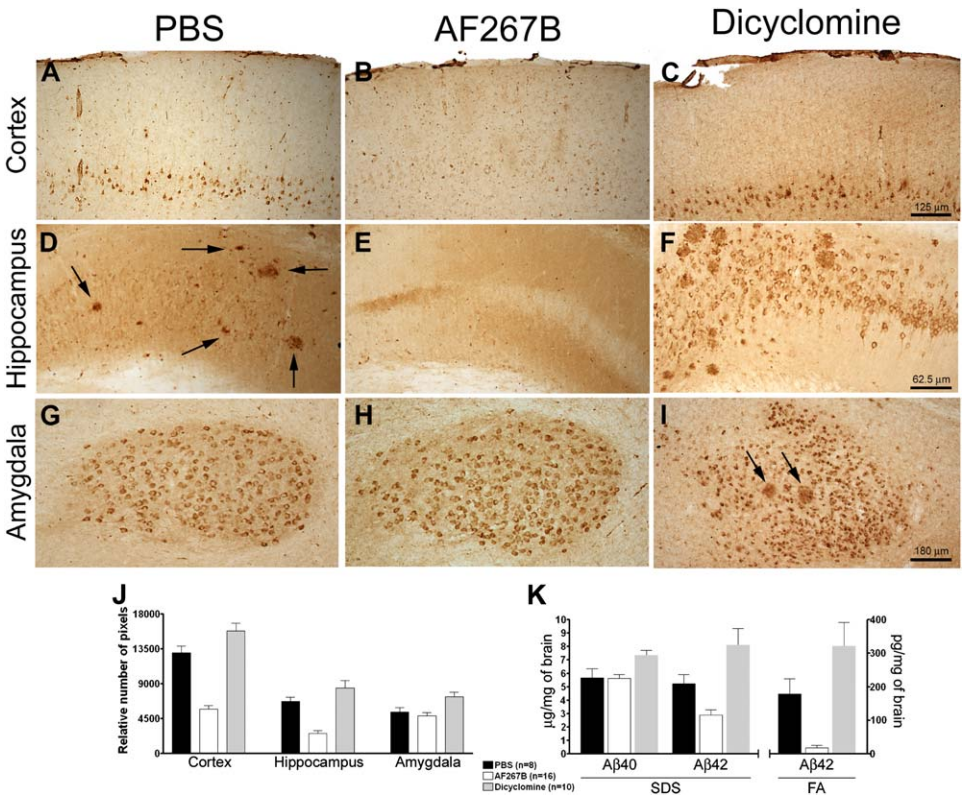

Figure 3. AF267B Reduces Aβ in the Cortex and Hippocampus

To determine the effects of AF267B and dicyclomine administration on the AD pathology present in the 3xTg-AD mice, we compared sections from PBS-, dicyclomine-, and AF267B-treated mice stained with an anti-Aβ1-42-specific antibody from Biosource (Camarillo, CA).

(A–F) AF267B significantly reduced the Aβ immunoreactivity in the cortex and hippocampus of treated mice, whereas dicyclomine led to an exacerbation of the Aβ pathology in the same brain regions. Arrows in panel (D) point to extracellular amyloid plaques.

(G–I) AF267B did not have any effects on the Aβ load in the amygdala; however, dicyclomine administration caused an increase in Aβ pathology in this brain region leading to the buildup of diffuse plaques (arrows in [I]).

(J) Represents the quantification analysis of panels (A)–(I), indicating a significant reduction of Aβ immunoreactivity in the cortex ($p < 0.001$, $t = 7.580$) and hippocampus ($p < 0.001$, $t = 4.738$) but not in the amygdala ($p > 0.05$, $t = 0.7025$) of AF267B-treated versus PBS-treated 3xTg-AD mice. Aβ immunoreactivity was, however, significantly higher in the cortex ($p < 0.05$, $t = 2.568$), hippocampus ($p < 0.05$, $t = 2.785$), and amygdala ($p < 0.05$, $t = 2.694$) of dicyclomine-treated mice compared to PBS-treated mice.

(K) To quantitatively determine the effect of AF267B and dicyclomine on Aβ levels, we used sandwich ELISA. In the SDS-soluble fraction, we did not observe any changes in the steady-state levels of $A\beta_{40}$ among all the groups ($p > 0.05$), whereas the levels of $A\beta_{42}$ were significantly reduced in the AF267B-treated mice and significantly increased in the dicyclomine-treated mice, compared to the PBS-treated mice ($p < 0.05$, $t = 2.750$; and $p < 0.05$, $t = 2.812$, respectively). We also observed a significant reduction in the steady-state levels of $A\beta_{42}$ in the formic acid extracted fraction following AF267B administration ($p < 0.05$, $t = 3.126$). In contrast, the levels of insoluble $A\beta_{42}$ were significantly higher in the brains of dicyclomine-treated 3xTg-AD mice ($p < 0.01$, $t = 4.062$). We did not detect any $A\beta_{40}$ in this fraction.

(Figure 5C). In vitro data suggest that stimulation of M1 receptors leads to an increase in the production of secreted αAPP (reviewed by Bigl and Rossner, 2003). This effect seems to be mediated by an activation of both PKC and ERK1/2. In fact, stimulation of M1 receptors in the presence of a PKC or ERK1/2 inhibitor reduces αAPP levels (Haring et al., 1998). Interestingly, the biggest reduction in the M1-mediated increase in α-APP was obtained when both PKC and ERK1/2 were blocked simultaneously (Haring et al., 1998). Similarly, direct activation of PKC leads to an increase in αAPP production; however, the PKC-mediated increase in αAPP was not present if the experiments were conducted in fibroblasts from ADAM17 knockout mice (Buxbaum et al., 1998). Taken together, these data suggest that AF267B modulates APP processing through the activation of both ERK1/2 and PKC, providing a mechanistic link between M1 receptor activation and APP processing in vivo.

AF267B Reduces tau Pathology in the Cortex and Hippocampus

To determine the effects of M1 agonist or antagonist on the tau pathology, we immunohistochemically evaluated sections from PBS-, dicyclomine-, and AF267B-treated 3xTg-AD mice with different anti-tau antibodies (Figures 6 and 7). At 8 months of age, the homozygous 3xTg-AD mice show tau immunoreactivity in the somatodendritic compartment of CA1 pyramidal neurons, in the cortex, and in the amygdala (see Figures 6A, 6J, and 6S). At this age, some CA1 neurons are also immunoreactive with AT8 (Figure 6D), whereas no AT8-positive neurons are detected at this age in the cortex or amygdala, and no PHF1-positive neurons are detected in any brain regions at this age (Figures 6G, 6M, 6P, 6V, and 6Y). Following chronic AF267B treatment, we observed a marked reduction of tau immunoreactivity in the somatodendritic compartment of cortical and

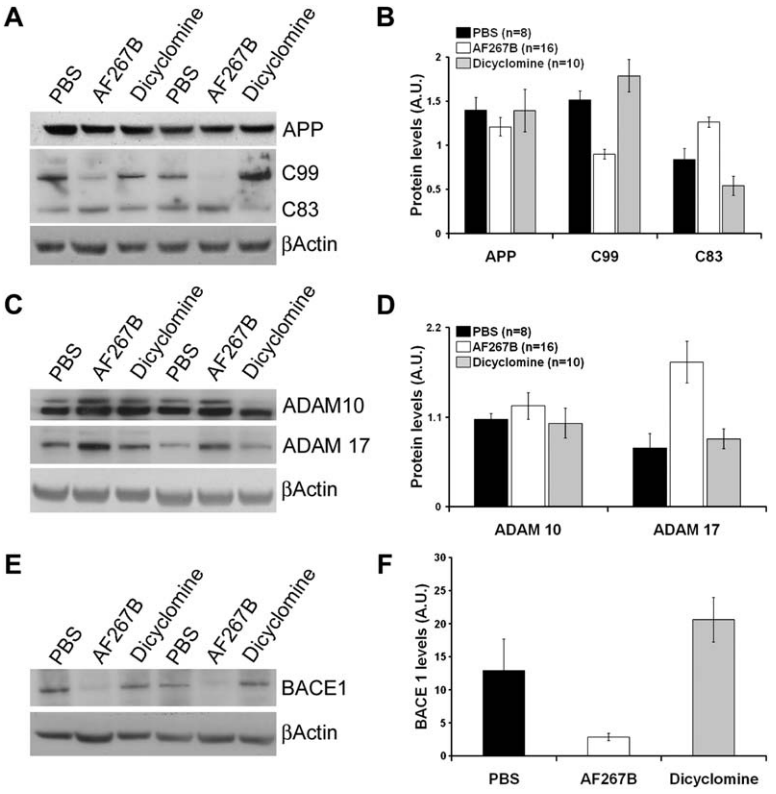

Figure 4. AF267B and Dicyclomine Inversely Modulate APP Processing

To determine the mechanism by which AF267B and dicyclomine modulate Aβ levels, we investigated APP processing. Panel (A) shows representative Western blots for APP holoportein, C99, and C83. (B) The quantification analysis shows that the steady-state levels of APP were not altered by either treatment, although there is a concomitant decrease in C99 levels with an increase in C83 levels in the AF267B-treated mice compared to PBS-treated mice ($p < 0.01$, $t = 3.804$; and $P < 0.01$, $t = 3.287$, respectively). Opposite results were obtained in the brains of dicyclomine-treated 3xTg-AD mice, with an increase in C99 levels and a significant decrease in C83 levels compared to AF267B-treated mice ($p < 0.001$, $t = 5.892$; and $p < 0.001$, $t = 6.018$). These results indicate that there is a shift in APP processing toward the nonamyloidogenic pathway. (C–F) We also measured the steady-state levels of ADAM10 and ADAM17, two putative α-secretase enzymes; and BACE1, a β-secretase enzyme. Panel (C) shows representative Western blots of steady-state levels of ADAM10 and ADAM17. The quantification analysis in panel (D) shows that AF267B and dicyclomine did not affect the levels of ADAM10 ($p > 0.05$); however, AF267B-treatment did cause a significant increase in the levels of ADAM17/TACE ($p < 0.05$, $t = 3.024$). In contrast, the levels of this enzyme were reduced in the brains of dicyclomine-treated mice relative to the AF267B-treated mice ($p < 0.05$, $t = 2.951$). Panel (E) shows a representative Western blot probed with a BACE1-specific antibody. Quantification analysis (F) shows that the steady-state levels of BACE1 are significantly decreased in AF267B-treated mice ($p < 0.01$, $t = 2.949$), whereas BACE1 levels were increased in the dicyclomine-treated mice. Although the levels of BACE1 were higher in the dicyclomine-treated mice versus the PBS-treated mice, this difference did not achieve statistical significance ($p > 0.05$, $t = 2.514$).

hippocampal neurons (Figures 6B, 6K, 7A, and 7B). Notably, we could no longer detect any AT8 staining in the hippocampus of the AF267B-treated 3xTg-AD mice (Figures 6D, 6E, 7D). In contrast, we found a significant increase in tau phosphorylation in the brains of dicyclomine-treated 3xTg-AD. In particular, the number of AT8- and PHF1-positive neurons were greatly increased in the hippocampus (Figures 6F, 6I, 7D, and 7G). Notably, dicyclomine administration accelerated the onset of tau pathology, as we could also detect PHF1-positive neurons in the cortex and amygdala of these mice (Figures 6R, 6AA, 7H, and 7I). Analogous to the Aβ pathology, AF267B treatment did not reduce the tau pathology in the amygdala, as the level of staining was comparable in the brain regions between PBS- and AF267B-treated 3xTg-AD mice (Figure 6S, 6T, 6V, 6W, 6Y, 6Z, 7C, 7F, and 7I). The changes in tau phosphorylation were also verified by quantitative Western blot analysis (Figures 8A and 8B).

To elucidate the mechanism underlying the reduction in tau pathology in AF267B-treated mice, we used quantitative Western blot analysis to screen a panel of candidate tau kinases, using antibodies against the activated form of these enzymes. We found that the steady-state levels of the active forms of GSK3α, p-38 MAPK, or CDK5 and its activators p25 and p35, were not significantly different among the groups analyzed (Figures 8A and 8C–8E and data not shown). GSK3β is another important kinase involved in tau phosphorylation, and using an antibody specific for the activated forms of GSK3β, we found a significant decrease in the levels of activated GSK3β in the brain of 3xTg-AD mice treated with AF267B compared to PBS-treated mice (Figures 8A and 8E). In contrast, dicyclomine treatment led to an increase in GSK3β, although the change was not statistically significant (Figures 8A and 8E). To further confirm the involvement of GSK3β in the cholinergic-modulated changes in tau phosphorylation, we directly measured the enzymatic activity of this enzyme. Compared to PBS-treated mice, the enzymatic activity of this enzyme was significantly decreased in the brains of AF267B-treated mice and significantly increased in the brains of dicyclomine-treated mice (Figure 8F). These data suggest that the decrease in tau phosphorylation induced by AF267B treatment is mediated by the reduction of GSK3β activity. Taken together, these data clearly show that modulating M1 activity can have pronounced consequences on the tau pathology: the M1 agonist AF267B reduces GSK3β activity whereas the M1 antagonist dicyclomine enhances it. These data are supported by previous in vitro studies showing that activation of M1 mAChRs can reduce GSK3β activity, by activating PKC (Forlenza et al., 2000). Moreover, we cannot exclude the possibility that some of the reduction in HT7 staining in the AF267B-treated mice is also due to the decrease in Aβ, as we previously showed

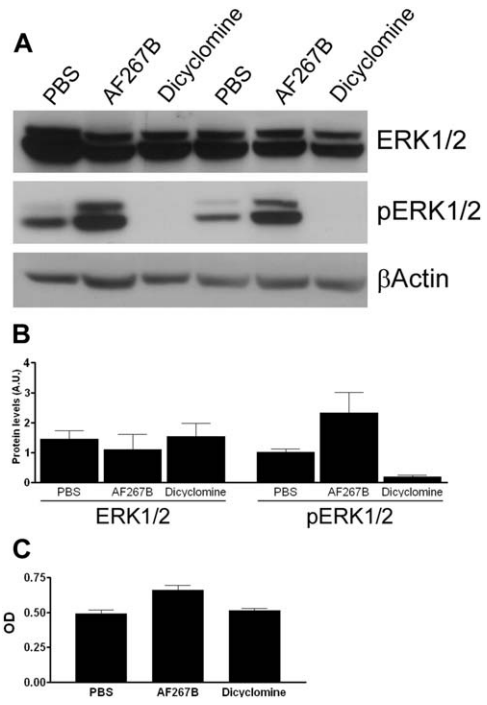

Figure 5. Increase in ERK1/2 and PKC Activities following AF267B Treatment

To elucidate the mechanism by which AF267B modulates APP processing, we measured the activity of ERK1/2 and PKC. Panel (A) shows representative Western blots probed with a ERK1/2-pan antibody, an antibody specific against phosphorylated ERK1/2 and β-Actin (used as a loading control). Panel (B) shows a quantitative analysis of the blots presented in (A) (n = 6/group). The total levels of ERK1/2 were not statistically significant among the three groups of 3xTg-AD mice ($p > 0.05$). In contrast, AF267B-treated mice had an increase in the activated form of ERK1/2 compared to PBS-treated mice ($p < 0.05$, $t = 3.017$). Moreover, the levels of activated ERK1/2 were greatly decreased in the dicyclomine-treated mice ($p < 0.01$, $t = 4.217$). Panel (C) shows the relative levels of PKC activity. AF267B administration leads to a significant increase in PKC activity ($p < 0.01$, $t = 3.901$). The activity of PKC was significantly reduced in the brains of dicyclomine-treated versus AF267B-treated 3xTg-AD mice ($p < 0.01$, $t = 3.659$). The number of mice analyzed for this experiment was as follows: PBS (n = 8), AF267B (n = 16), dicyclomine (n = 10).

the lowering Aβ reduces HT7-positive, nonphosphorylated tau (Oddo et al., 2004).

Discussion

This study identifies the selective M1 agonist AF267B as a peripherally administered low molecular weight compound that effectively reduces the two major hallmark neuropathological lesions and rescues the cognitive deficits in an animal model of AD. Previous work has shown that activation of M1 mAChRs leads to the generation of α-secretase-generated products (Allinson et al., 2003; Buxbaum et al., 1992; Haring et al., 1998; Nitsch et al., 1992). We find that the same effect holds true in the 3xTg-AD mice, as the mechanism underlying the reduction of Aβ is mediated through enhanced steady-state levels of ADAM17/TACE, the inducible α-secretase (Allinson et al., 2003; Buxbaum et al., 1998), whereas this treatment lowers BACE1 levels. Several in vitro studies have suggested that PKC and ERK1/2 underlie the M1 receptor-mediated effect on APP processing (Bigl and Rossner, 2003). In particular it has been shown that activation of PKC and ERK1/2 is necessary to modulate APP-processing by activating M1 receptors (Haring et al., 1998). We have shown that PKC and ERK1/2 activities are indeed increased following AF267B administration, clearly suggesting that the mechanism by which AF267B increases ADAM17 activity is mediated by PKC and ERK1/2. Consistent with our results are the in vitro data showing that a direct activation of PKC leads to an increase in the production of αAPP, a process mediated by ADAM17, as activation of PKC in fibroblast from ADAM17 knockout mice failed to increase αAPP production (Buxbaum et al., 1998).

We further showed that the selective M1 agonist also attenuates the tau pathology, as we detected a significant reduction in the somatodendritic compartmentalization of tau as well as reduced AT8-immunoreactivity in the AF267B-treated 3xTg-AD mice. The mechanism underlying the decrease in GSK3β activity in the AF267B-treated mice appears to involve enhanced PKC activity, a finding that agrees well with other studies (Forlenza et al., 2000; Nitsch et al., 1993). Moreover, because we previously showed that lowering Aβ levels via immunotherapy can also lead to a reduction in the tau pathology (Oddo et al., 2004), we cannot exclude the possibility that the lower Aβ levels caused by AF267B also contribute to the lower tau pathology.

A major goal of the next generation of AD therapies is to identify disease-modifying compounds rather than simply treating the disease symptoms. In this regard, AF267B clearly meets this criterion, at least in an animal model, by effectively shifting APP processing away from the amyloidogenic pathway and by reducing the activity of a major tau kinase, GSK3β. Equally significant, we also find that a relatively short, 10 week treatment with AF267B rescues the behavioral deficit in the 3xTg-AD mice. The improved cognitive function is closely linked with the reduction of the Aβ and tau pathology in this model. We observed a reduction in these two pathological hallmarks in the hippocampus and cortex, and this is associated with improved cognitive performance in a hippocampal-dependent task. In contrast, AF267B had no impact upon the Aβ and tau pathology in the amygdala, and likewise, performance on passive inhibitory avoidance, a behavioral task mainly dependent on the amygdala, was not improved with treatment. The lack of reduction of the Aβ pathology in the amygdala is likely not a reflection of the fact that M1 receptors are expressed at lower levels in the amygdala compared to hippocampus and cortex (Spencer et al., 1986). As we have shown, the effect on Aβ is likely mediated by ADAM17/TACE, which, as previously shown, is highly expressed in the cortex and hippocampus but not in the amygdala (Karkkainen et al., 2000). Therefore, the lower expression of this enzyme in the amygdala may be accountable for the lack of effect of AF267B on Aβ pathology in this brain region. ADAM17/TACE was previously reported to be colocalized with amyloid plaques in AD brains and it was suggested to have an important role as an antagonist of Aβ production by competing with BACE1 for APP cleavage (Skovronsky et al.,

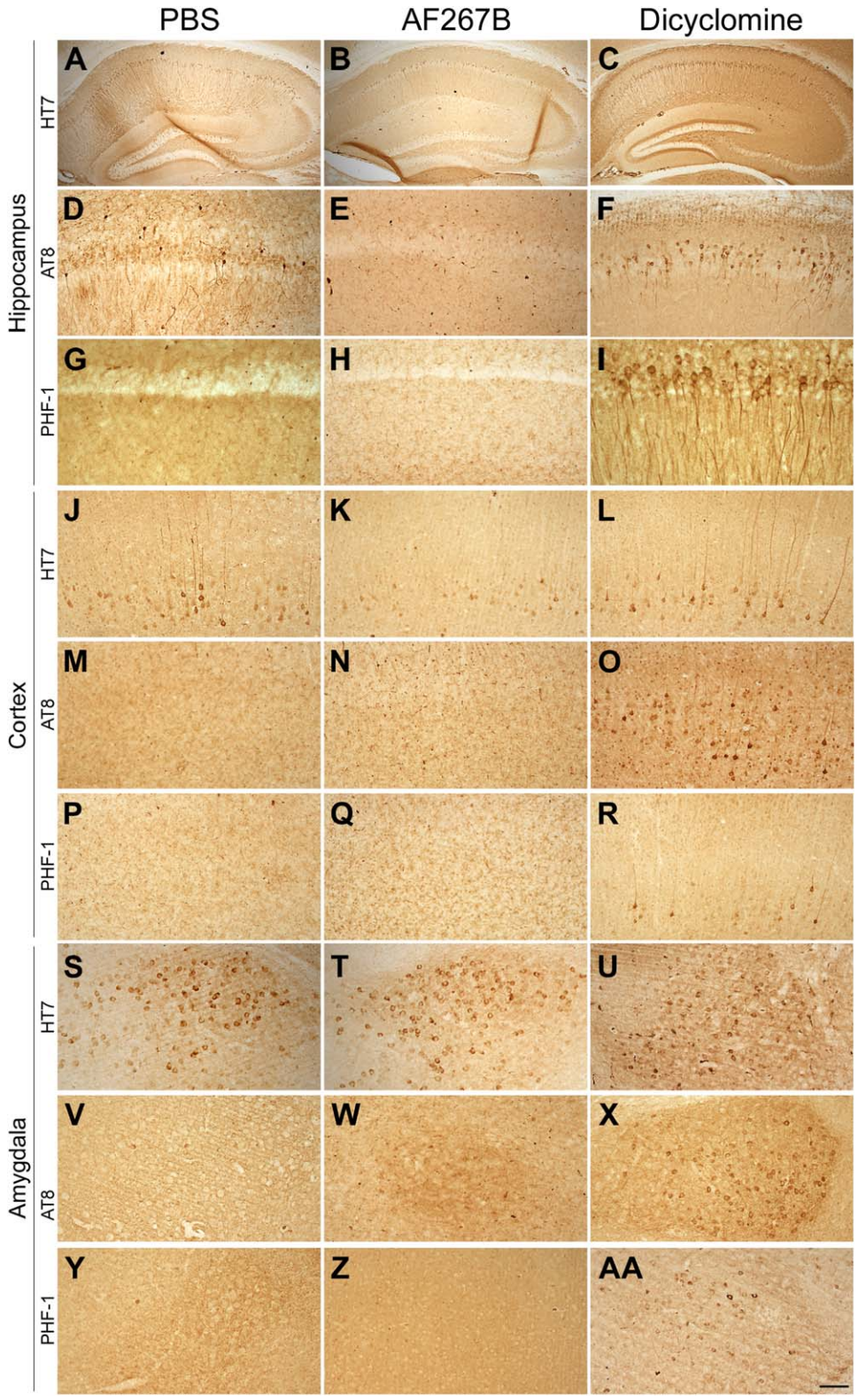

Figure 6. AF267B Reduces tau Pathology in the Cortex and Hippocampus

To determine the effects of AF267B and dicyclomine on the tau pathology, we stained brain sections from PBS-, AF267B-, and dicyclomine-treated 3xTg-AD mice. (A–C) Somatodendritic tau deposits in the hippocampus are significantly reduced following AF267B treatment; however, an increase in HT7 immunoreactivity is detected in the brains of the dicyclomine-treated mice. (D–F) AT8-positive neurons were not detectable in the hippocampus of AF267B-treated mice, whereas a marked increase was found in the hippocampus of dicyclomine-treated mice. (G–I) PHF1-positive neurons were not observed in the brains of PBS- and AF267B-treated mice, whereas readily apparent PHF1-positive neurons were found in the hippocampus of the dicyclomine-treated mice. (J–R) As we previously reported, AT8- or PHF1-positive neurons are not routinely

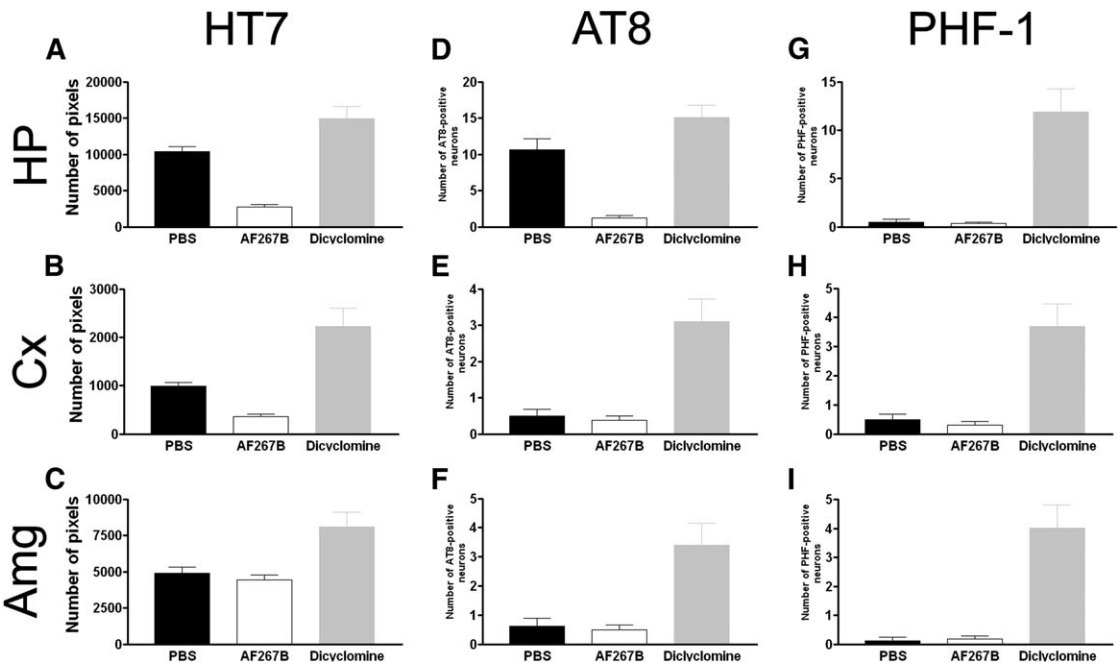

Figure 7. Quantitative Assessment of the tau Pathology in the Hippocampus, Cortex, and Amygdala of PBS-, AF267B-, and Dicyclomine-Treated Mice

(A–C) Quantification analysis of brain sections stained with HT7 shows a significant reduction in the tau load following AF267B treatment compared to PBS-treated mice in the hippocampus (A) and cortex (B) ($p < 0.001$, $t = 5.797$; and $p < 0.05$, $t = 3.190$, respectively). In the amygdala, however, the tau load was unchanged between these two groups (C). In contrast, the tau load was significantly increased in the hippocampus, cortex, and amygdala of dicyclomine-treated mice compared to PBS-treated mice ($p < 0.05$, $t = 2.941$; $p < 0.01$, $t = 3.939$; $p < 0.01$, $t = 3.4$).

(D–I). The number of AT8-positive neurons was greatly reduced in the hippocampus of AF267B-treated versus PBS-treated 3xTg-AD mice (D) ($p < 0.001$, $t = 5.97$). No tau phosphorylation at the AT8 or PHF-1 site is detected in the cortex (E and H) and amygdala (F and I) of PBS- and AF267B-treated mice. The number of AT8- and PHF-1-positive neurons was significantly higher in the hippocampus, cortex, and amygdala of dicyclomine-treated mice compared to PBS-treated mice (D–I). For AT8 in the hippocampus, cortex, and amygdala, the p and t values were: $p < 0.05$, $t = 2.601$; $p < 0.001$, $t = 4.787$; $p < 0.001$, $t = 4.196$, respectively. For PHF-1 in the hippocampus, cortex, and amygdala, the p and t values were: $p < 0.001$, $t = 5.887$; $p < 0.001$, $t = 4.868$; $p < 0.001$, $p = 5.809$, respectively.

Number of mice analyzed for this study: PBS treatment, n = 8; AF267B treatment, n = 16; dicyclomine treatment, n = 10. HP, hippocampus; Cx, cortex; Amg, amygdala.

2001). In this context, AF267B may represent a novel therapeutic strategy in AD, by shifting the balance of APP processing toward the nonamyloidogenic pathway.

The loss of cholinergic activity is an invariant feature of AD, and inhibiting cholinesterase activity continues to be a mainstay of current AD-based treatments (Ibach and Haen, 2004). Although anticholinesterases produce some short-term benefits to patients, these agents lose their efficacy over time, probably because they are not disease-modifying agents. Other pharmacological strategies, such as the use of nAChR and mAChR agonists, may represent another means for activating cholinergic receptors in the AD brain. In this regard, we previously showed that activation of nAChRs by chronic nicotine exposure exacerbates tau pathology in the 3xTg-AD mice by activating p38-MAP kinases (Oddo et al., 2005). In contrast, the results of the present study show the remarkable therapeutic potential of AF267B in attenuating the major hallmark neuropathological lesions relevant to AD and in restoring cognitive function, at least for certain tasks. It is also remarkable that administration of dicyclomine exacerbates the Aβ and tau pathology, reinforcing the positive role of M1 mAChRs in modulating these pathological hallmarks of AD. Further work, including clinical trials in humans, will be necessary to determine if this new generation of M1 agonists will produce a similar therapeutic efficacy as was observed in the 3xTg-AD mice.

Experimental Procedures

Compounds Used

AF267B [(S)-2-ethyl-8-methyl-1-thia-4,8-diazaspiro[4.5]decan-3-one] was synthesized in the laboratory of Dr. Fisher (US Pat. 5,852,029). The batch used in the present study was >99.9% pure, as determined by chiral and achiral HPLC (data not shown). The

observed in the cortex of 6- to 8-month-old 3xTg-AD mice (J and K, M and N, P and Q). The HT7 immunoreactivity was decreased in the brains of AF267B-treated versus PBS-treated mice (K). In contrast, we found a marked increase in HT7-, AT8-, and PHF1-positive neurons following dicyclomine treatment in the same brain regions (L, O, and R). (S–AA) AF267B did not alter the tau pathology in the amygdala ($p > 0.05$). HT7 immunoreactivity was increased in the amygdala of dicyclomine-treated mice compared to PBS- and AF267B-treated mice (S–U). As for the cortex, no AT8 or PHF-1 immunoreactivity is detectable in the amygdala of 8-month-old 3xTg-AD mice (V and W, Y and Z). In contrast, we found some AT8- and PHF1-positive neurons in the amygdala of dicyclomine-treated mice (X–AA). The scale bar is 250 μm for (A)–(C), 125μm for (D)–(F) and (J)–(AA), 62.5 μm for (G)–(I).

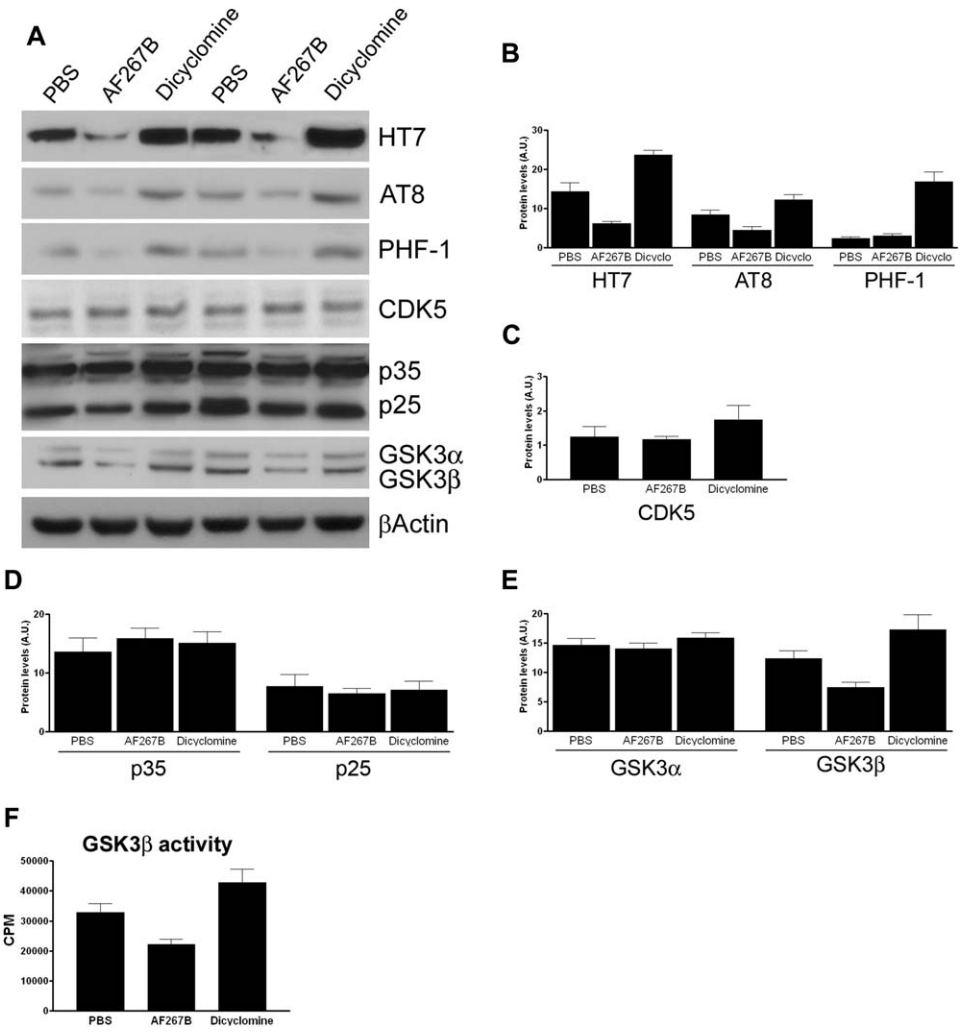

Figure 8. AF267B Reduces GSK3β Activity

(A and B) The changes in tau levels and phosphorylation after AF267B or dicyclomine treatment were confirmed by Western blot (A and B). Quantitative assessment of the Western blots was done by one-way ANOVA followed by a Bonferroni post-test comparison. Total tau levels were significantly reduced in the brains of AF267B-treated mice versus PBS-treated mice ($p < 0.001$, $t = 5.322$) and significantly increased in the brains of dicyclomine-treated mice compared to both PBS- and AF267B-treated mice ($p < 0.001$, $t = 5.444$ and $p < 0.001$, $t = 12.73$, respectively). AT8 tau levels were significantly decreased in the AF267B brains compared to PBS-treated mice ($p < 0.05$, $t = 2.6$). In contrast, AT8 levels were significantly increased following dicyclomine treatment compared to AF267B-treated mice ($p < 0.001$, $t = 5.429$). The PHF-1 levels were significantly higher in the brains of dicyclomine-treated mice compared to PBS- and AF267B-treated mice ($p < 0.001$, $t = 7.217$ and $p < 0.001$, $t = 7.966$, respectively). To determine the mechanism by which AF267B and dicyclomine modulate tau phosphorylation, we measured the steady-state levels of several tau kinases. Panel (A) shows a representative Western blot probed with a CDK5, p35, and a specific anti-GSK3 antibody that recognizes the activated form of GSK3β (pY216).

(C–E) The levels of CDK5 and its activators p35 and p25, and the levels of GSK3α were not changed following AF267B or dicyclomine administration. However, AF267B treatment selectively reduced the steady-state levels of the activated form of GSK3β ($p < 0.05$, $t = 3.019$) (E). In contrast, there was a significant increase in the levels of GSK3β in the brains of dicyclomine-treated 3xTg-AD mice ($p < 0.05$, $t = 3.194$).

(F) We next directly measured the enzymatic activity of GSK3β. We found that the activity of this enzyme was decreased following AF267B administration ($p < 0.05$, $t = 2.833$), whereas it was increased following dicyclomine administration ($p < 0.05$, $t = 3.214$).

The number of mice used for these experiments was as follow: PBS, n = 8; AF267B, n = 16; dicyclomine, n = 10.

chemical structure of the compound is presented in Figure S1. Dicyclomine was purchased from Sigma, St. Louis, MO (Cat # D-7909).

Mice, Treatment, and Behavioral Tests

The derivation and characterization of the 3xTg-AD mice has been described elsewhere (Oddo et al., 2003). Briefly, two independent transgenes encoding human APP_{Swe} and the human tau_{P301L} (both under control of the mouse Thy1.2 regulatory element) were comicroinjected into single-cell embryos harvested from homozygous mutant $PS1_{M146V}$ knockin (PS1-KI) mice (Oddo et al., 2003). For the AF267B studies, 6-month-old homozygous 3xTg-AD and age-matched NonTg mice were chronically injected i.p. with either AF267B [(S)-2-ethyl-8-methyl-1thia-4,8-diazaspiro[4.5]decan-3-one] or PBS. For the dicyclomine studies, 6-month-old homozygous 3xTg-AD and age-matched NonTg mice were chronically injected via i.p. with dicyclomine (Sigma). All mice were given ad libitum access to food and water. A detailed description of the behavioral tests used here was previously described (Billings et al., 2005).

Antibodies

The following antibodies were used: anti-Aβ 6E10, anti-Aβ 1560 (both raised against amino acids 1–17 of Aβ), anti-Aβ1-42, anti-APP

22C11 (raised against amino acid 66–81 of APP), anti-Tau HT7 (raised against amino acids 159–163), AT8 (recognizes phosphorylated Ser202, Thr205), anti-GSK3β-pY216, anti-β-actin, anti-p38 (which recognizes phosphorylated Thr180 and Tyr182), anti-CDK5 (which recognizes amino acids 268–283), anti M1 mAChRs (raised against amino acids 269–320), anti BACE1 (raised against amino acids 485–501), ADAM10 (raised against amino acids 732–748), and anti-ADAM17 (raised against amino acid 807–823), anti-phosphorylated ERK1/2 at residues T185/Y187, and panERK1/2 antibody (Biosource, Camarillo, CA).

Protein Extraction, Immunohistochemistry, and Western Blot

Mice were sacrificed by CO_2 asphyxiation, and their brains were cut in half sagitally. One-half of the brain was fixed for 48 hr in 4% paraformaldehyde in TBS for immunohistochemical analysis. The other half was frozen in dry ice for biochemical analysis. 50 μm thick free-floating sections were obtained using a vibratome slicing system. A detailed immunostaining procedure has been previously described (Oddo et al., 2005). The primary antibodies were applied at the following dilutions: 1:1000 for 6E10, 1:3000 for 1560, 1:200 for Aβ42, 1:1000 for HT7, 1:200 for AT8.

For biochemical analysis, brains were homogenized in a solution of 2% SDS in H_2O containing 0.7 mg/ml Pepstatin A supplemented with complete Mini protease inhibitor tablet and phosphatase inhibitors 1:100. The homogenized mixes were sonicated to sheer the DNA and centrifuged at 4ºC for 1 hr at 100,000 × g. The supernatant was stored as soluble fraction. The pellet was rehomogenized in 70% formic acid (FA) and centrifuged as above. The supernatant was stored as the insoluble fraction. Proteins from the soluble fraction were resolved using standard Western blot techniques, as previously described (Oddo et al., 2005).

Aβ and tau Quantification

To quantify the changes in Aβ and tau immunoreactivity, photomicrographs (three sections/mouse, three photographs/section) were taken with a Zeiss digital camera and imported into the Scion Image system (NIH) and converted to black and white images. Threshold intensity was manually set and kept constant, and the number of pixels was determined for Aβ and tau immunostained sections.

ELISA

Aβ1-40 and Aβ1-42 levels were measured using a sensitive sandwich ELISA system. Proteins from the soluble fraction (see above) were loaded directly onto ELISA plates, and FA fractions were diluted 1:20 in neutralization buffer (1 M Tris base; 0.5 M NaH_2PO dibasic) prior to loading. MaxiSorp immunoplates (Nalge Nunc International, Rochester, NY) were coated with monoclonal antibody 20.1, a specific antibody against $Aβ_{1-16}$ (from Dr. W.E. Van Nostrand, Stony Brook University, NY) in coating buffer (0.1 M $NaCO_3$ [pH 9.6]), and blocked with 3% BSA. Synthetic Aβ standards (Bachem, King of Prussia, PA) were defibrillated by dissolving in hexafluoroisopropanol (HFIP) at 1 mg/ml and the HFIP evaporated with a stream of N_2. The defibrillated Aβ was dissolved in DMSO at 1 mg/ml. Standards of both Aβ1-40 and Aβ1-42 were made in antigen capture buffer (ACB; 20 mM NAH_2PO_4, 2 mM EDTA, 0.4 M NaCl, 0.5 g CHAPS, 1% BSA [pH 7.0]) and loaded onto ELISA plates in duplicate. Samples were loaded in duplicate and incubated overnight at 4ºC. Plates were washed and probed with either HRP-conjugated anti-Aβ 35-40 (MM32-13.1.1, for $Aβ_{40}$) or anti-Aβ 35-42 (MM40-21.3.4, for $Aβ_{42}$) overnight at 4ºC. 3,3′,5,5′-tetramethylbenzidine was used as the chromagen, and the reaction was stopped with the addition of 30% O-phosphoric acid and read at 450 nm on a plate reader (Labsystems, Sunnyvale, CA).

PKC and GSK3β Activities

PKC activity was measured using a kit from Streegen (Victoria, Canada) in accordance with the manufacturer's instructions. GSK3β activity was measured as previously described (Kitazawa et al., 2005).

Statistics

Behavior scores were analyzed using a multifactor or repeated-measures ANOVA including genotype and/or probe trial (1.5 hr and 24 hr). Post hoc Scheffe tests were used to determine individual differences in groups with respect to controls (NonTg mice and PBS-treated 3xTg-AD mice). All the other data were analyzed using one-way analyses of variance (ANOVA) with Bonferroni post test using GraphPad Prism version 3.00 for Windows (GraphPad Software, San Diego, CA). All the data analyses were conducted in a blinded fashion.

Supplemental Data

The Supplemental Data for this article can be found online at http://www.neuron.org/cgi/content/full/49/5/671/DC1/.

Acknowledgments

This work was supported by a grant to F.M.L. from the NIA (AG0212982) and the Alzheimer's Association (IIRG-02-3767).

Received: August 26, 2005
Revised: December 9, 2005
Accepted: January 12, 2006
Published: March 1, 2006

References

Allinson, T.M., Parkin, E.T., Turner, A.J., and Hooper, N.M. (2003). ADAMs family members as amyloid precursor protein alpha-secretases. J. Neurosci. Res. *74*, 342–352.

Bigl, V., and Rossner, S. (2003). Amyloid precursor protein processing in vivo–insights from a chemically-induced constitutive overactivation of protein kinase C in Guinea pig brain. Curr. Med. Chem. *10*, 871–882.

Billings, L.M., Oddo, S., Green, K.N., McGaugh, J.L., and Laferla, F.M. (2005). Intraneuronal Abeta causes the onset of early Alzheimer's disease-related cognitive deficits in transgenic mice. Neuron *45*, 675–688.

Buxbaum, J.D., Oishi, M., Chen, H.I., Pinkas-Kramarski, R., Jaffe, E.A., Gandy, S.E., and Greengard, P. (1992). Cholinergic agonists and interleukin 1 regulate processing and secretion of the Alzheimer beta/A4 amyloid protein precursor. Proc. Natl. Acad. Sci. USA *89*, 10075–10078.

Buxbaum, J.D., Liu, K.N., Luo, Y., Slack, J.L., Stocking, K.L., Peschon, J.J., Johnson, R.S., Castner, B.J., Cerretti, D.P., and Black, R.A. (1998). Evidence that tumor necrosis factor alpha converting enzyme is involved in regulated alpha-secretase cleavage of the Alzheimer amyloid protein precursor. J. Biol. Chem. *273*, 27765–27767.

Cuajungco, M.P., Faget, K.Y., Huang, X., Tanzi, R.E., and Bush, A.I. (2000). Metal chelation as a potential therapy for Alzheimer's disease. Ann. N Y Acad. Sci. *920*, 292–304.

Davies, P., and Maloney, A.J. (1976). Selective loss of central cholinergic neurons in Alzheimer's disease. Lancet *2*, 1403.

DeMattos, R.B., Bales, K.R., Cummins, D.J., Dodart, J.C., Paul, S.M., and Holtzman, D.M. (2001). Peripheral anti-A beta antibody alters CNS and plasma A beta clearance and decreases brain A beta burden in a mouse model of Alzheimer's disease. Proc. Natl. Acad. Sci. USA *98*, 8850–8855.

Eglen, R.M., Choppin, A., and Watson, N. (2001). Therapeutic opportunities from muscarinic receptor research. Trends Pharmacol. Sci. *22*, 409–414.

Forlenza, O.V., Spink, J.M., Dayanandan, R., Anderton, B.H., Olesen, O.F., and Lovestone, S. (2000). Muscarinic agonists reduce tau phosphorylation in non-neuronal cells via GSK-3beta inhibition and in neurons. J. Neural Transm. *107*, 1201–1212.

Giachetti, A., Giraldo, E., Ladinsky, H., and Montagna, E. (1986). Binding and functional profiles of the selective M1 muscarinic receptor antagonists trihexyphenidyl and dicyclomine. Br. J. Pharmacol. *89*, 83–90.

Hardy, J., and Selkoe, D.J. (2002). The amyloid hypothesis of Alzheimer's disease: progress and problems on the road to therapeutics. Science *297*, 353–356.

Haring, R., Fisher, A., Marciano, D., Pittel, Z., Kloog, Y., Zuckerman, A., Eshhar, N., and Heldman, E. (1998). Mitogen-activated protein

kinase-dependent and protein kinase C-dependent pathways link the m1 muscarinic receptor to beta-amyloid precursor protein secretion. J. Neurochem. *71*, 2094–2103.

Ibach, B., and Haen, E. (2004). Acetylcholinesterase inhibition in Alzheimer's Disease. Curr. Pharm. Des. *10*, 231–251.

Jankowsky, J.L., Savonenko, A., Schilling, G., Wang, J., Xu, G., and Borchelt, D.R. (2002). Transgenic mouse models of neurodegenerative disease: opportunities for therapeutic development. Curr. Neurol. Neurosci. Rep. *2*, 457–464.

Janus, C., Phinney, A.L., Chishti, M.A., and Westaway, D. (2001). New developments in animal models of Alzheimer's disease. Curr. Neurol. Neurosci. Rep. *1*, 451–457.

Karkkainen, I., Rybnikova, E., Pelto-Huikko, M., and Huovila, A.P. (2000). Metalloprotease-disintegrin (ADAM) genes are widely and differentially expressed in the adult CNS. Mol. Cell. Neurosci. *15*, 547–560.

Kitazawa, M., Oddo, S., Yamasaki, T.R., Green, K.N., and LaFerla, F.M. (2005). Lipopolysaccharide-induced inflammation exacerbates tau pathology by a cyclin-dependent kinase 5-mediated pathway in a transgenic model of Alzheimer's disease. J. Neurosci. *25*, 8843–8853.

Lammich, S., Kojro, E., Postina, R., Gilbert, S., Pfeiffer, R., Jasionowski, M., Haass, C., and Fahrenholz, F. (1999). Constitutive and regulated alpha-secretase cleavage of Alzheimer's amyloid precursor protein by a disintegrin metalloprotease. Proc. Natl. Acad. Sci. USA *96*, 3922–3927.

Levey, A.I., Kitt, C.A., Simonds, W.F., Price, D.L., and Brann, M.R. (1991). Identification and localization of muscarinic acetylcholine receptor proteins in brain with subtype-specific antibodies. J. Neurosci. *11*, 3218–3226.

McGaugh, J.L., McIntyre, C.K., and Power, A.E. (2002). Amygdala modulation of memory consolidation: interaction with other brain systems. Neurobiol. Learn. Mem. *78*, 539–552.

Muir, J.L. (1997). Acetylcholine, aging, and Alzheimer's disease. Pharmacol. Biochem. Behav. *56*, 687–696.

Nitsch, R.M., Slack, B.E., Wurtman, R.J., and Growdon, J.H. (1992). Release of Alzheimer amyloid precursor derivatives stimulated by activation of muscarinic acetylcholine receptors. Science *258*, 304–307.

Nitsch, R.M., Slack, B.E., Farber, S.A., Borghesani, P.R., Schulz, J.G., Kim, C., Felder, C.C., Growdon, J.H., and Wurtman, R.J. (1993). Receptor-coupled amyloid precursor protein processing. Ann. N Y Acad. Sci. *695*, 122–127.

Nordberg, A., and Winblad, B. (1986). Reduced number of [3H]nicotine and [3H]acetylcholine binding sites in the frontal cortex of Alzheimer brains. Neurosci. Lett. *72*, 115–119.

Nordberg, A., Alafuzoff, I., and Winblad, B. (1992). Nicotinic and muscarinic subtypes in the human brain: changes with aging and dementia. J. Neurosci. Res. *31*, 103–111.

Nordberg, A., Hellstrom-Lindahl, E., Lee, M., Johnson, M., Mousavi, M., Hall, R., Perry, E., Bednar, I., and Court, J. (2002). Chronic nicotine treatment reduces beta-amyloidosis in the brain of a mouse model of Alzheimer's disease (APPsw). J. Neurochem. *81*, 655–658.

Oddo, S., Caccamo, A., Shepherd, J.D., Murphy, M.P., Golde, T.E., Kayed, R., Metherate, R., Mattson, M.P., Akbari, Y., and LaFerla, F.M. (2003). Triple-transgenic model of Alzheimer's disease with plaques and tangles: intracellular Abeta and synaptic dysfunction. Neuron *39*, 409–421.

Oddo, S., Billings, L., Kesslak, J.P., Cribbs, D.H., and LaFerla, F.M. (2004). Abeta immunotherapy leads to clearance of early, but not late, hyperphosphorylated tau aggregates via the proteasome. Neuron *43*, 321–332.

Oddo, S., Caccamo, A., Green, K.N., Liang, K., Tran, L., Chen, Y., Leslie, F.M., and LaFerla, F.M. (2005). Chronic nicotine administration exacerbates tau pathology in a transgenic model of Alzheimer's disease. Proc. Natl. Acad. Sci. USA *102*, 3046–3051.

Pinnix, I., Musunuru, U., Tun, H., Sridharan, A., Golde, T., Eckman, C., Ziani-Cherif, C., Onstead, L., and Sambamurti, K. (2001). A novel gamma-secretase assay based on detection of the putative C-terminal fragment-gamma of amyloid beta protein precursor. J. Biol. Chem. *276*, 481–487.

Postina, R., Schroeder, A., Dewachter, I., Bohl, J., Schmitt, U., Kojro, E., Prinzen, C., Endres, K., Hiemke, C., Blessing, M., et al. (2004). A disintegrin-metalloproteinase prevents amyloid plaque formation and hippocampal defects in an Alzheimer disease mouse model. J. Clin. Invest. *113*, 1456–1464.

Riekkinen, P., Jr., Schmidt, B.H., and van der Staay, F.J. (1998). Animal models in the development of symptomatic and preventive drug therapies for Alzheimer's disease. Ann. Med. *30*, 566–576.

Rosenblum, K., Futter, M., Jones, M., Hulme, E.C., and Bliss, T.V. (2000). ERKI/II regulation by the muscarinic acetylcholine receptors in neurons. J. Neurosci. *20*, 977–985.

Schenk, D., Barbour, R., Dunn, W., Gordon, G., Grajeda, H., Guido, T., Hu, K., Huang, J., Johnson-Wood, K., Khan, K., et al. (1999). Immunization with amyloid-beta attenuates Alzheimer-disease-like pathology in the PDAPP mouse. Nature *400*, 173–177.

Selkoe, D.J. (2001). Alzheimer's disease: genes, proteins, and therapy. Physiol. Rev. *81*, 741–766.

Skovronsky, D.M., Fath, S., Lee, V.M., and Milla, M.E. (2001). Neuronal localization of the TNFalpha converting enzyme (TACE) in brain tissue and its correlation to amyloid plaques. J. Neurobiol. *49*, 40–46.

Spencer, D.G., Jr., Horvath, E., and Traber, J. (1986). Direct autoradiographic determination of M1 and M2 muscarinic acetylcholine receptor distribution in the rat brain: relation to cholinergic nuclei and projections. Brain Res. *380*, 59–68.

Sugaya, K., Giacobini, E., and Chiappinelli, V.A. (1990). Nicotinic acetylcholine receptor subtypes in human frontal cortex: changes in Alzheimer's disease. J. Neurosci. Res. *27*, 349–359.

Sugden, P.H., and Clerk, A. (1997). Regulation of the ERK subgroup of MAP kinase cascades through G protein-coupled receptors. Cell. Signal. *9*, 337–351.

Vassar, R., Bennett, B.D., Babu-Khan, S., Kahn, S., Mendiaz, E.A., Denis, P., Teplow, D.B., Ross, S., Amarante, P., Loeloff, R., et al. (1999). Beta-secretase cleavage of Alzheimer's amyloid precursor protein by the transmembrane aspartic protease BACE. Science *286*, 735–741.

Wei, J., Walton, E.A., Milici, A., and Buccafusco, J.J. (1994). m1-m5 muscarinic receptor distribution in rat CNS by RT-PCR and HPLC. J. Neurochem. *63*, 815–821.

Whitehouse, P.J., Martino, A.M., Antuono, P.G., Lowenstein, P.R., Coyle, J.T., Price, D.L., and Kellar, K.J. (1986). Nicotinic acetylcholine binding sites in Alzheimer's disease. Brain Res. *371*, 146–151.

Woolf, N.J. (1996). The critical role of cholinergic basal forebrain neurons in morphological change and memory encoding: a hypothesis. Neurobiol. Learn. Mem. *66*, 258–266.